

1 **Controls on stable isotope and trace metal uptake in**
2 ***Neogloboquadrina pachyderma* (sinistral) from an Antarctic**
3 **sea-ice environment**

4
5 Katharine R. Hendry¹, Rosalind E.M. Rickaby¹, Michael P. Meredith² & Henry Elderfield³
6
7

8 ¹Department of Earth Sciences, University of Oxford, Parks Road, Oxford, OX1 3PR,
9 UK

10

11 ²British Antarctic Survey, High Cross, Madingley Road, Cambridge, CB3 0ET, UK

12

13 ³Department of Earth Sciences, University of Cambridge, Downing Street, Cambridge,
14 CB2 3EQ, UK

15 ***Abstract***

16 The polar foraminifera *Neogloboquadrina pachyderma* (sinistral) dominates assemblages from
17 the high latitude Southern Ocean, which is a key region for paleoclimate studies. Here,
18 we use *N. pachyderma* (s.) harvested from sediment traps off the West Antarctic Peninsula
19 to construct a seasonal time series for the calibration of calcite proxies in a high latitude
20 seasonal sea-ice environment where temperature is decoupled from other environmental
21 parameters. We have used a combination of $\delta^{18}\text{O}_{\text{CaCO}_3}$ and $\delta^{13}\text{C}_{\text{CaCO}_3}$ to decipher the
22 calcification temperature and salinity, which reflect that *N. pachyderma* (s.) live in surface
23 waters throughout the year, and at the ice-water interface in austral winter. Further, our
24 results demonstrate that, during winter, the uptake of trace metals into *N. pachyderma* (s.)
25 calcite is influenced by secondary environmental conditions in addition to temperature

26 during periods of sea-ice. We suggest an elevated carbonate ion concentration at the ice-
27 water interface resulting from biological utilisation CO_2 could influence calcification in
28 foraminifera. We demonstrate that for *N. pachyderma* (s.) Mg/Ca and Sr/Ca ratios are
29 linear functions of calcification temperature and $[\text{CO}_3^{2-}]$. *N. pachyderma* (s.) Mg/Ca ratios
30 exhibit temperature sensitivity similar to previous studies ($\sim 10\%$ per $^\circ\text{C}$) and a
31 sensitivity to $[\text{CO}_3^{2-}]$ of $\sim 1\%$ per $\mu\text{mol kg}^{-1}$. Sr/Ca ratios are less sensitive to
32 environmental parameters, exhibiting $< 1\%$ increase per $^\circ\text{C}$ and per $10\ \mu\text{mol kg}^{-1}$. We
33 show how a multi-proxy approach could be used to constrain past high latitude surface
34 water temperature and $[\text{CO}_3^{2-}]$.

35

36 Keywords: *N. pachyderma*; isotopes; trace metals; sea-ice; carbonate ion

37

38 **1 Introduction**

39 Atmospheric gases trapped in bubbles within ice cores show the partial pressure of
40 carbon dioxide (pCO_2) was 80 ppmV lower during the Last Glacial Maximum (LGM)
41 compared with modern values (Siegenthaler et al., 2005). Of the many hypotheses
42 proposed to account for this CO_2 shift, a significant focus has been placed on past
43 changes in productivity, chemistry and circulation in the Southern Ocean (Anderson et
44 al., 2002; Sigman and Boyle, 2000). Accordingly, there is a clear motivation to obtain
45 reliable information about these processes in the past Southern Ocean. The stable
46 isotopic and trace metal composition of planktonic foraminiferal calcite provide
47 important geochemical tools for reconstructing past changes in sea surface conditions.
48 In particular, *Neogloboquadrina pachyderma* (sinistral) is a species of interest as it dominates
49 modern planktonic assemblages in the high latitudes and Southern Ocean sediments.
50 However, inference of past calcification conditions from *N. pachyderma* (s.) chemistry can

51 be ambiguous, in part because the species can live in a variety of habitats, including sea-
52 ice. Open water *N. pachyderma* (s.) are generally considered pycnocline dwellers, but can
53 calcify below the mixed layer, occupying a wide range of depths shallower than 200 m
54 (Kohfeld et al., 1996). In sea-ice conditions, *N. pachyderma* (s.) are associated in high but
55 patchy cell concentrations with the bottom community of sea-ice diatoms, which grows
56 in the more porous layers at the ice-water interface (Lipps and Krebs, 1974). In the
57 autumn, the adults conduct gametogenesis, such that juveniles appear in the upper part
58 of the water column and become incorporated into the forming frazil ice (Spindler and
59 Dieckmann, 1986).

60 There is an increasing appreciation that multiple factors control stable isotope and trace
61 metal chemistry of foraminifera. In particular, the role of carbonate ion concentration,
62 $[\text{CO}_3^{2-}]$, and salinity on the uptake of trace metals (Mg, Sr and Li) into planktonic
63 foraminiferal calcite is not fully understood (Ferguson et al., 2008; Lea et al., 1999;
64 Marriott et al., 2004; Mortyn et al., 2005; Russell et al., 2004). Further, Southern Ocean
65 waters are undersaturated with respect to calcite such that foraminifera have a low
66 preservation potential in slowly accumulating sediments. This, in turn, means that there
67 is a paucity of calibration studies involving high latitude species in the literature. Here,
68 we present a multi-proxy calibration study of *N. pachyderma* (s.) from the West Antarctic
69 Peninsula (WAP) collected using sediment traps. We use the stable isotopic composition
70 of the calcite to determine where the foraminifera calcify and to demonstrate that trace
71 metal uptake depends on factors other than temperature and salinity, such as $[\text{CO}_3^{2-}]$,
72 during periods of sea-ice cover. We have calculated $[\text{CO}_3^{2-}]$ from measurements of
73 Dissolved Inorganic Carbon (DIC) and pH for a limited period of the year, and inferred
74 $[\text{CO}_3^{2-}]$ throughout the year using B/Ca ratios and shell weights, which agree on a
75 consistent change in $[\text{CO}_3^{2-}]$ at the depth of calcification throughout the year. This
76 allows other trace metal proxies, Mg/Ca, Sr/Ca and Li/Ca, to be calibrated for

77 temperature and $[\text{CO}_3^{2-}]$ using linear regression. Our multi-proxy approach potentially
78 allows temperature and $[\text{CO}_3^{2-}]$ effects to be deconvolved, such that these parameters can
79 be constrained in the past using high latitude foraminifera from marine sediment cores.

80 **2 Materials and methods**

81 A set of moorings was deployed in Marguerite Bay, WAP, in January 2005 from the
82 British Antarctic Survey vessel RRS James Clark Ross (840 m water depth). The site is
83 close to the Rothera Oceanographic and Biological Time-Series (RaTS) site (Clarke et al.,
84 2008) (Figure 1), an on-going programme featuring quasi-weekly water column profiling
85 and discrete water sampling. The mooring comprised a suite of oceanographic
86 instrumentation, including a sediment trap at 200 m with bottle closure times configured
87 to sample sinking particles throughout the year at fortnightly to bimonthly periods (Table
88 1). The bottles were pre-loaded with 2% buffered formalin to preserve organic material.
89 The sediment trap bottles were recovered the following year and stored at 4°C.
90 Foraminifera were picked from the sediment trap splits by K. Weston (University of East
91 Anglia, UK). *N. pachyderma* (s.) specimens were present in sediment trap bottles from
92 summer to winter months, confirming their presence in the water column throughout the
93 year. The foraminiferal organic matter and calcite were well preserved and some
94 individuals were present connected as growth chains, which suggests insignificant
95 transport in the water column.

96
97 Light microscopy, Scanning Electron Microscopy (SEM) imaging and probe analysis
98 were used to assess the microstructural scale preservation of one or two foraminifera per
99 trap bottle. Light microscope analyses show these sediment trap foraminifera are
100 “glassy” rather than “frosty” (Sexton et al., 2006) and SEM images confirm they are well
101 preserved without either dissolution due to calcite undersaturation or secondary calcite

102 precipitation (Figure 2). Energy Dispersive Spectrometry (EDS) shows Al, Mg and Fe
103 levels are below detection implying no surface contamination. Foraminifera shell size
104 was estimated by eye (compared to sieved *N. pachyderma* fractions) and was found to
105 occupy a narrow size range (~ 212-300 μm). Encrusted specimens (Figure 2B) were not
106 included in analysis to avoid any contribution from secondary or gametogenic calcite,
107 which may have a different chemical composition to the other calcite layers (Brown and
108 Elderfield, 1996; Eggins et al., 2003; Elderfield and Ganssen, 2000; Kohfeld et al., 1996;
109 Ni et al., 2007; Nurnberg et al., 1996; Sadekov et al., 2005).

110 Total shell weights were measured ($\pm 1 \mu\text{g}$) and the mean weight calculated per shell. The
111 shell sizes and weights are typical of cold water *N. pachyderma* (s.) from open water and
112 sea-ice (Barker and Elderfield, 2002; Donner and Wefer, 1994; Spindler and Dieckmann,
113 1986).

114 The oxygen and carbon isotopic composition of five to six foraminifera ($> 250 \mu\text{m}$) per
115 bottle were analysed using a VG Isogas Prism II mass spectrometer with an on-line VG
116 Isocarb common acid bath preparation system (Oxford University). Samples are first
117 cleaned for organic matter using hydrogen peroxide and acetone and dried at 60°C for at
118 least 30 minutes. In the instrument they are reacted with purified phosphoric acid at
119 90°C . Calibration to Pee Dee Belemnite (PDB) standard via NBS-19 is made daily using
120 the Oxford in-house (NOCZ) Carrara marble standard. Reproducibility of replicated
121 standards is usually better than 0.1‰ for $\delta^{13}\text{C}$ and $\delta^{18}\text{O}$.

122

123 There was insufficient material to analyse different size fractions for trace metals, so the
124 remaining foraminifera were crushed gently between two clean glass plates and cleaned
125 for clays by sonicating in $18 \text{ M}\Omega$ water. The process was repeated two more times with
126 $18 \text{ M}\Omega$ water and twice with reagent grade methanol.

127 *Oxidising stage*

128 Due to the nature of the sediment trap samples, the oxidising stage of the foraminifera
129 cleaning procedure was adapted for higher organic matter content (Anand et al., 2003).
130 0.25 ml of 50% H₂O₂ (made up with 0.2 M NaOH, making a final solution of 0.1 M
131 NaOH) was added to each sample and placed in a hot water bath (70 °C) for a total of 45
132 minutes, and the samples rinsed twice with 18 MΩ water.

133 *Final weak acid leach, dissolution and analysis*

134 100-250 ml quartz distilled (QD) 0.001 N HNO₃ was added to each sample, sonicated
135 and supernatant removed. This was repeated up to four times, and finally rinsed with
136 QD water. The samples were dissolved on the day of analysis using 250 ml QD 0.1 N
137 HNO₃, sonicated, centrifuged to settle any remaining particles and transferred to a clean
138 tube for analysis. Trace metal analysis was carried out by Q-ICP-MS (University of
139 Cambridge), which have been tested by an interlaboratory comparison study by M.
140 Greaves and J. Yu using external, matrix-matched standards (Rosenthal et al., 2004).
141 Long term reproducibility is 1.4% for Mg/Ca, 0.9% for Sr/Ca, 2.4% for Li/Ca and 4.2%
142 for B/Ca ratios (Yu et al., 2005).

143 *δ¹⁸O_{water} of the water column*

144 As part of RaTS, full-depth profiles of temperature and salinity were collected at the
145 shallow mooring site on a quasi-weekly basis, using a SeaBird SBE19 conductivity-
146 temperature-depth (CTD) sensor. Profiling was conducted from a small boat during
147 summer and through a hole cut in the ice during winter. Discrete water samples were
148 drawn from 15 m depth using a Niskin bottle closed with a messenger weight. These
149 were sealed for transportation to the UK for oxygen isotope analysis. In addition, full-
150 depth profiles of oxygen isotopes were obtained each December as part of hydrographic
151 casts conducted during visits of RRS James Clark Ross to Rothera. Full details of the
152 RaTS CTD profiling procedures and data quality, oxygen isotope analysis methods and

153 data are described elsewhere (Clarke et al., 2008; Meredith et al., 2008; Meredith et al.,
154 2004).

155 **3 Results and discussion**

156 **3.1 Reconstructing foraminiferal habitat from stable isotopes**

157 In order to understand the controls on trace metal uptake into *N. pachyderma* (s.), it is
158 essential to constrain the depth and ambient environmental conditions at calcification.
159 Here we define the foraminifera habitat using the $\delta^{18}\text{O}_{\text{CaCO}_3}$ and $\delta^{13}\text{C}_{\text{CaCO}_3}$, which can be
160 combined with RaTS CTD profiles to determine calcification temperature and salinity.

161 ***3.1.1 Calcification depth from $\delta^{18}\text{O}$***

162 *a) Simulating $\delta^{18}\text{O}_{\text{water}}$ profiles*

163 We can use $\delta^{18}\text{O}_{\text{CaCO}_3}$, with the Shackleton paleotemperature equation, to determine
164 habitat depth because vertical profiles for both temperature and $\delta^{18}\text{O}_{\text{water}}$ are available for
165 Marguerite Bay. Stable isotopic values for the calcite range from 0.66 to 1.48 ‰ and 2.60
166 to 3.26 ‰ for $\delta^{13}\text{C}$ and $\delta^{18}\text{O}$ respectively (Table 1; Figure 3). Measured $\delta^{18}\text{O}_{\text{water}}$ range
167 from -0.2 to -0.8 ‰, with more depleted values observed in surface waters. Typically,
168 isotopically lighter waters occur near the surface during the austral fall ($\delta^{18}\text{O}_{\text{water}} \sim -0.8$
169 ‰), with isotopically heavier waters found during the austral spring ($\delta^{18}\text{O}_{\text{water}} \sim -0.5$ to -
170 0.6 ‰), reflecting the seasonal cycles in precipitation, glacial melt and sea-ice/upper
171 ocean processes (Meredith et al., 2008). A simulated full-depth $\delta^{18}\text{O}_{\text{water}}$ field was
172 produced from the approximately weekly time series of discrete samples taken at 15 m
173 depth and the full-depth $\delta^{18}\text{O}_{\text{water}}$ profiles collected during December of each year. For
174 this, the quasi-linear relationship between salinity and $\delta^{18}\text{O}_{\text{water}}$ for Marguerite Bay was

175 used along with the approximately weekly full-depth salinity and temperature profiles
 176 that were collected at the same time as the $\delta^{18}\text{O}_{\text{water}}$ samples (Meredith et al., 2008). The
 177 Mixed Layer Depth (MLD) to which the upper water column is homogenised by surface
 178 processes was derived from each of the weekly profiles, and all values within the mixed
 179 layer were set to the $\delta^{18}\text{O}_{\text{water}}$ value at 15 m for each cast. Beneath the mixed layer,
 180 $\delta^{18}\text{O}_{\text{water}}$ from the full-depth casts was regressed on salinity, and this was used to convert
 181 the measured salinity from the weekly profiles into simulated $\delta^{18}\text{O}_{\text{water}}$ piecewise in 50 m
 182 sections. Combined, this produced full-depth $\delta^{18}\text{O}_{\text{water}}$ profiles at approximately weekly
 183 intervals (Figure 5a).

184 *b) Predicting $\delta^{18}\text{O}_{\text{CaCO}_3}$*

185 The $\delta^{18}\text{O}_{\text{CaCO}_3}$ was predicted using Shackleton's 1974 equation and assuming the
 186 simulated values of $\delta^{18}\text{O}_{\text{water}}$:

$$187 \quad \left(\delta^{18}\text{O}_{\text{CaCO}_3}\right)_{\text{pred}} = \left\{ \delta^{18}\text{O}_{\text{water}} + 21.9 - \sqrt{310.61 + 10T} \right\} - v \quad (1)$$

188 where v is a correction factor to account for vital effects. The $\delta^{18}\text{O}_{\text{water}}$ values were
 189 corrected to PDB using Equation 2 (Bemis et al., 1998):

$$190 \quad \delta^{18}\text{O}_{\text{water}} = 0.9998 \times \delta^{18}\text{O}_{\text{SMOW}} - 0.2 \quad (2)$$

191 For *N. pachyderma* (s.) the vital offset has been estimated as between 0.5 and 1.3 ‰
 192 (Bauch et al., 1997; Kohfeld et al., 2000; Ortiz et al., 1996; Simstich et al., 2003; Smith et
 193 al., 2005; Volkmann, 2000). A temperature dependent vital offset based on measured
 194 ambient $\delta^{18}\text{O}_{\text{water}}$ (Bauch et al., 1997) was used with RaTS site sea-surface temperatures to
 195 correct the $\delta^{18}\text{O}_{\text{CaCO}_3}$ measurements (Table 2). The vital offsets are similar between
 196 Arctic (Bauch et al., 1997) and Antarctic *N. pachyderma* (s.) (Kohfeld et al., 1996; Mortyn
 197 and Charles, 2003) despite evidence for cryptic speciation (Darling et al., 2007). The
 198 associated error is estimated to be ± 0.2 ‰.

199 *c) Reconstructing calcification depths*

200 Although the error on the vital effect is relatively large, the depth of calcification can be
201 estimated by matching the measured and predicted values of $\delta^{18}\text{O}_{\text{CaCO}_3}$ (Figure 5b, c).
202 Furthermore, we can derive the temperature and salinity from the CTD profiles in order
203 to calibrate the trace metal proxies with ambient environmental conditions at the depth
204 of calcification. Although this is relatively straightforward in sea-ice free months, it is
205 more difficult to assign ambient salinity values in winter given the foraminifera may be
206 living in the sea-ice brine channels or at the ice-water interface (Lipps and Krebs, 1974).
207 Sea-ice formation does not affect $\delta^{18}\text{O}_{\text{water}}$ significantly, so will have only a minor
208 influence on $\delta^{18}\text{O}_{\text{CaCO}_3}$ (Weiss et al., 1979). However, the extent of open exchange
209 between the sea-ice habitat and the underlying seawater, and thus the ambient salinity,
210 can be determined using the carbon isotopic composition of the foraminiferal calcite.

211 ***3.1.2 Winter sea-ice habitat from $\delta^{13}\text{C}$***

212 The primary controls on $\delta^{13}\text{C}_{\text{CaCO}_3}$ are the carbon isotopic composition of DIC in the
213 ambient water, the organic matter on which the foraminifera feed, temperature and
214 $[\text{CO}_3^{2-}]$ (Kohfeld et al., 2000). The $\delta^{13}\text{C}_{\text{DIC}}$ is lighter in winter than in summer as a result
215 of reduced gas exchange with the atmosphere due to sea-ice cover (Lynch-Stieglitz et al.,
216 1995). As the sea-ice becomes persistent, gas exchange with the atmosphere is effectively
217 shut off, and the $\delta^{13}\text{C}_{\text{CaCO}_3}$ values become depleted by $\sim 0.8\text{‰}$ (Table 1). As the air
218 temperature rises to -5 to -9°C , the sea-ice breaches the porosity threshold (Golden et al.,
219 1998; Perovich et al., 2004) and becomes an open, interconnected system allowing the
220 replenishment of lighter carbon from the seawater interface. Increased gas exchange
221 with the atmosphere enriches the carbon isotopic composition of DIC, organic matter
222 and foraminiferal calcite (Delille et al., 2007).

223 The carbon isotopic composition of the food source will depend on where the
224 foraminifera are feeding, particularly in winter. $\delta^{13}\text{C}_{\text{org}}$ values from sea-ice brine algae
225 collected from the isotopically closed upper layers of sea-ice by sackhole drilling are
226 heavier than surface water values due to Rayleigh fractionation of carbon during
227 biological utilisation in a closed system (Gibson et al., 1999; Carson et al., in prep).
228 However, the observed variations in $\delta^{13}\text{C}_{\text{CaCO}_3}$ here suggest that the dietary $\delta^{13}\text{C}_{\text{org}}$ does
229 not become significantly heavier from summer to winter (Figure 3), and that the
230 foraminifera are feeding in a system openly exchanging with the underlying water.
231 Furthermore, if the foraminifera lived in the less consolidated bottom layers of platelet
232 ice they would be more likely to escape the sea-ice and sink to the sediment traps. It is
233 reasonable, therefore, to assume that during winter the foraminifera analysed lived at the
234 ice-water interface and experienced surface water temperatures and salinities that remain
235 relatively constant at the inferred foraminiferal habitat throughout the year (Figure 5b).

236 **3.2 Controls on trace metal uptake in *N.pachyderma* (s.)**

237 The Mg/Ca, Sr/Ca, B/Ca and Li/Ca ratios vary between 0.77-1.06 mmol/mol, 1.37-1.41
238 mmol/mol, 50-75 $\mu\text{mol/mol}$ and 17.4-19.8 $\mu\text{mol/mol}$ respectively (Figure 4). The trace
239 metal seasonal profiles show a peak in austral winter, which is not observed in the
240 surface temperature profile or stable isotopic composition (Figure 3, 4; Table 1). We have
241 inferred from the isotopic composition of the calcite that the foraminifera calcify at the
242 ice-water interface, suggesting against any temperature, salinity or Rayleigh fractionation
243 effects on foraminifera chemistry. If our assumption is correct, it would suggest that
244 there is some additional factor influencing calcification during the period of sea-ice cover,
245 such as $[\text{CO}_3^{2-}]$. Here, we will reconstruct the ambient $[\text{CO}_3^{2-}]$ of the calcifying
246 foraminifera, before discussing the effect on tract metal uptake.

247 **3.3.1 Shell weight and boron uptake**

248 Culture experiments have shown stable isotope and trace metal uptake into planktonic
249 foraminifera may also be a function of $[\text{CO}_3^{2-}]$, in addition to temperature and salinity
250 (Russell et al., 2004; Spero et al., 1997). Although the carbonate system was not fully
251 constrained throughout the year in Marguerite Bay, we have calculated $[\text{CO}_3^{2-}]$ from
252 available data of Dissolved Inorganic Carbon (DIC) and pH measured at the RaTS site
253 (Carson et al., in prep). $[\text{CO}_3^{2-}]$ values are calculated using a simple speciation model
254 (carbcalc 5e, Boyle, 2005) for seawater at 15 m depth and brine from upper sea-ice layers
255 collected by sackhole drilling.

256 We infer in the previous section that the winter habitat of *N.pachyderma* (s.) is at the ice-
257 water interface, which likely represents the chemical transition between the low $[\text{CO}_3^{2-}]$ of
258 the surface waters and the extremely high $[\text{CO}_3^{2-}]$ of the closed system upper layers of
259 sea-ice. Qualitatively, therefore, the effect of the presence of sea-ice on the growth
260 habitat of *N.pachyderma* (s.) is to elevate ambient $[\text{CO}_3^{2-}]$ (Figure 6). Quantitatively, we
261 can infer $[\text{CO}_3^{2-}]$ at the site of calcification from shell weights (Barker and Elderfield,
262 2002) and the B/Ca ratio (Yu et al., 2007). We cannot use the predictable relationship
263 between temperature and $[\text{CO}_3^{2-}]$ in open seawater in the Southern Ocean (King and
264 Howard, 2004) because it is unlikely to hold in seasonal sea-ice environments. Both sea-
265 ice and the ice-water interface are known to exhibit undersaturation of CO_2 as a result of
266 biological activity and brine expulsion (Delille et al., 2007; Gleitz et al., 1995;
267 Papadimitiou et al., 2007), leading to a decoupling between $[\text{CO}_3^{2-}]$ and temperature.

268 The mean shell weights range from $\sim 6 \mu\text{g}$ per shell to $\sim 14 \mu\text{g}$ per shell (Figure 6). The
269 pristine nature of the foraminifera suggests variability in the shell weight profile, also
270 reflected in the shell geochemistry, is a result of environmental conditions rather than
271 dissolution or encrustation effects (Figure 2). Specifically, there is a peak in midwinter

272 between June and October, where shell weights increase $\sim 4 \mu\text{g}$ per shell (Figure 6).
273 According to the calibration of Barker & Elderfield (2002) this shell weight change
274 corresponds to an increase in $[\text{CO}_3^{2-}]$ of $\sim 40 \mu\text{mol kg}^{-1}$ (note though that this calibration
275 is for *N. pachyderma* (dextral)). This feature is unrelated to changes in the contribution of
276 different size fractions (Figure 6), which suggests the geochemical variation is not a
277 function of shell size or ontogeny.

278 B/Ca, thought to be a measure of $[\text{CO}_3^{2-}]$, is a relatively new proxy (Foster, 2008; Yu and
279 Elderfield, 2005; Yu et al., 2007). Boron is taken up into foraminifera calcite as the borate
280 ion ($\text{B}(\text{OH})_4^-$) (Hemming & Hansen, 1992), which exchanges with boric acid as a
281 function of pH resulting in both the B/Ca ratio and B isotopic fractionation (Yu et al.,
282 2007). The borate ion substitutes for CO_3^{2-} in the calcite lattice according to Equation 3:

$$283 \left(\frac{[\text{Ca}(\text{HBO}_3)]}{[\text{CaCO}_3]} \right) = K_D \left(\frac{[\text{B}(\text{OH})_4^-]}{[\text{HCO}_3^-]} \right) \quad (3)$$

284 Hence, as $[\text{HCO}_3^-]$ decreases (i.e. $[\text{CO}_3^{2-}]$ increases), $\text{B}(\text{OH})_4^-$ uptake increases (Gaillardet
285 and Allègre, 1995).

286 In this study, B/Ca shows a strong peak in mid-winter, which we suggest occurs at a time
287 when there are neither significant temperature nor salinity changes in the water column at
288 the depth of calcification (Figure 6). There is no change in the B/Ca ratio during the
289 period of cooling into winter, suggesting there is no significant temperature effect here
290 on boron uptake into calcite. This contradicts other studies that have shown a
291 temperature dependence on B uptake into foraminiferal calcite (Yu et al., 2007).
292 However, the water temperature variation experienced here is low (approximately 2°C),
293 suggesting that other factors dominate in this case.

294 The B/Ca ratio has been shown in other plankonic foraminifera (*Globigerinoides inflata*) to
295 relate to $[\text{CO}_3^{2-}]$ according to Equation 4 (Yu et al., 2007), where the numbers in
296 parentheses show 95% confidence intervals.

297 $[CO_3^{2-}] = 0.8647(\pm 0.16)(B/Ca) + 108.29(\pm 11.2)$ (4)

298 Although there are thought to be species-specific dependence on B incorporation into
299 foraminiferal calcite, the latitudinal trend and range in B/Ca ratios for *G. inflata* and *N.*
300 *pachyderma* (s.) are similar (Yu, pers. com.). Hence, in the absence of a published
301 calibration, we have used the *G. inflata* relationship (Equation 4) to reconstruct temporal
302 changes in $[CO_3^{2-}]$ in Marguerite Bay (Figure 6).

303 The B/Ca data indicate an increase in $[CO_3^{2-}]$ (decrease in PCO_2) in the winter during the
304 period of sea-ice coverage of 30-40 $\mu\text{mol kg}^{-1}$. Whilst it is possible that the temperature
305 and $[CO_3^{2-}]$ effect could compensate each other at certain times of year, a peak in $[CO_3^{2-}]$
306 at the site of calcification inferred from the B/Ca ratios is consistent with the calculated
307 $[CO_3^{2-}]$ and shell weight variations (Figure 6).

308 In summary, the shell weight and B/Ca ratios are consistent with the foraminifera living
309 at the ice-water interface over winter. Sea-ice and the ice-water interface are known to
310 exhibit undersaturation of CO_2 as a result of biological activity and expulsion (Delille et
311 al., 2007; Gleitz et al., 1995; Papadimitiou et al., 2007; Figure 6), leading to the mid-
312 winter increase in $[CO_3^{2-}]$. We suggest the extremely high $[CO_3^{2-}]$ calculated for the upper
313 layers in sea-ice are not matched by the predictions from shell weights and B/Ca because
314 the degree of CO_2 utilisation is less extreme at the ice-water interface where the
315 foraminifera calcify. The change in $[CO_3^{2-}]$ is likely to change foraminiferal oxygen
316 isotopes by less than 0.1 ‰ (Spero et al., 1997), consistent with our $\delta^{18}O_{CaCO_3}$ variations
317 (Figure 3; Table 1), but may have an influence on trace metal uptake.

318

319 ***3.3.2 Carbonate ion effect on trace metal uptake***

320 Mg/Ca, Sr/Ca and Li/Ca ratios share similar “w-shaped” profiles, including both high
321 summer values and a midwinter peak also observed in the shell weight and B/Ca ratio

322 profiles, which suggests metal uptake is controlled by multiple environmental controls
323 including calcification temperature and $[\text{CO}_3^{2-}]$. Here, the sensitivity of Mg/Ca, Sr/Ca
324 and Li/Ca ratios to the different environmental parameters can be estimated and
325 constrained by linear regression with calcification temperature and $[\text{CO}_3^{2-}]$. Although the
326 Mg/Ca ratio is generally assumed to be an exponential function of calcification
327 temperature (Elderfield and Ganssen, 2000), the model here focuses on the low
328 temperature domain and so a linear approximation is valid.

329 Moving averages of calcification temperature and $[\text{CO}_3^{2-}]$, calculated from $\delta^{18}\text{O}_{\text{CaCO}_3}$ and
330 the B/Ca ratio respectively (Figure 6), were used to solve Equations 5-6 by fit of least
331 mean squares for Mg/Ca and Sr/Ca ratios (Figure 7).

$$332 \quad \frac{\text{Mg}}{\text{Ca}} = 0.11(\pm 0.02)T + 0.011(\pm 0.002)[\text{CO}_3^{2-}] - 0.69(\pm 0.2)$$

$$333 \quad r^2 = 0.33 \text{ (n=13, p<0.05)}$$

334 (5)

$$335 \quad \frac{\text{Sr}}{\text{Ca}} = 0.008(\pm 0.002)T + 0.0015(\pm 0.0002)[\text{CO}_3^{2-}] + 1.14(\pm 0.25)$$

$$336 \quad r^2 = 0.57 \text{ (n=13, p<0.05)}$$

337 (6)

338 There is no significant relationship between the predicted and measured Mg/Ca when
339 the linear regression is carried out for T and $[\text{CO}_3^{2-}]$ separately ($r^2 < 0.1$). Unfortunately,
340 there are not sufficient data points to conduct rigorous statistical testing, but
341 uncertainties have been estimated by optimising the sum of the least mean squares by
342 varying each parameter in turn to $\pm 5\%$ of the optimal value. (Note: this method does not
343 produce a good fit for Li/Ca ratios, $r^2 < 0.1$). A positive correlation between Mg/Ca
344 residuals and shell weight, an independent measure of $[\text{CO}_3^{2-}]$, provides further evidence
345 for a significant $[\text{CO}_3^{2-}]$ effect on *N. pachyderma* (s.) trace metal uptake (Figure 8).

346 Although further work is required to produce a rigorous calibration, our data can be used
347 to estimate the sensitivity of *N. pachyderma* (s.) calcite Mg/Ca and Sr/Ca ratios to
348 temperature and [CO₃²⁻]. The Mg/Ca ratios in this environment show similar
349 temperature sensitivity (~ 10 % per °C) to open water *N. pachyderma* (Elderfield and
350 Ganssen, 2000; Nurnberg, 1995; von Langen et al., 2005). Although some laboratory
351 and field studies suggest a salinity effect on Mg/Ca ratios (Ferguson et al., 2008), such an
352 effect cannot be tested here as there is little variability in calcification salinity. Sr/Ca is
353 less sensitive to environmental conditions than the Mg/Ca ratio (< 1% increase per °C
354 and per 10 μmol kg⁻¹) (Figure 7). This is consistent with previous culture experiments,
355 plankton tow and core top samples of non-globorotaliid foraminifera that demonstrate a
356 weak temperature effect on Sr uptake into planktonic foraminiferal calcite and an
357 increase in the Sr/Ca ratio with increasing pH (Mortyn et al., 2005; Russell et al., 2004).

358 *Implications for glacial-interglacial SST reconstructions*

359 The influence on *N. pachyderma* (s.) Mg/Ca ratios (and the uptake of other trace metals)
360 by environmental parameters other than temperature (e.g. [CO₃²⁻]) has implications for
361 glacial-interglacial SST reconstructions in regions where sea-ice cover varies on similar
362 timescales. This includes:

- 363 1) Regions of the subantarctic Southern Ocean that are outside the modern Seasonal Sea-
364 Ice Zone (SIZ) but were within the winter sea-ice extent during cooler periods;
- 365 2) Regions of coastal Antarctica that are within the modern SIZ but were covered by
366 multi-year ice during cooler periods.

367 Downcore records from the subantarctic Pacific indicate a change in *N. pachyderma* (s.)
368 Mg/Ca ratio of ~ 0.2 mmol/mol on a glacial-interglacial timescale (Mashiotta et al.,
369 1999), which is of similar amplitude to seasonal changes from this study. Diatom
370 population analysis (Gersonde et al., 2005) indicate that the core was near the edge of the
371 LGM winter sea-ice extent, such that the site may have experienced seasonal variation in

372 [CO₃²⁻] in the absence of temperature variation. The time averaging of such seasonality
373 in sediments requires further investigation for the robust interpretation of Southern
374 Ocean foraminiferal trace metal proxies.

375 **4 Summary and conclusions**

376 Here, we constrain the controls on geochemical proxies based on the high latitude
377 planktonic foraminifera, *Neogloboquadrina pachyderma* (s.) using time series sediment trap
378 samples from the West Antarctic Peninsula. $\delta^{18}\text{O}_{\text{CaCO}_3}$ and $\delta^{13}\text{C}_{\text{CaCO}_3}$ can be used to
379 demonstrate that the foraminifera calcify at the ice-water interface in winter, which
380 exchanges openly with seawater, and to reconstruct calcification temperature and salinity.
381 Our results show that trace metal uptake during calcification is influenced by factors
382 other than ambient temperature and salinity, especially during periods of sea-ice cover.
383 We suggest, using B/Ca ratios and shell weight data, that there is an increase in [CO₃²⁻]
384 during periods of sea-ice cover and that Mg/Ca, Sr/Ca and Li/Ca ratios are functions of
385 temperature and [CO₃²⁻]. *N. pachyderma* (s.) Mg/Ca exhibits similar temperature
386 sensitivity to previous studies (~ 10 % per °C) and a [CO₃²⁻] sensitivity of ~ 10 % per 10
387 $\mu\text{mol kg}^{-1}$. Sr/Ca is less sensitive to environmental parameters, exhibiting < 1% increase
388 per °C and per 10 $\mu\text{mol kg}^{-1}$. Seasonal variation in habitat, and associated changes in
389 ambient conditions with depth in the water column and the ice-water interface, adds a
390 further degree of uncertainty to paleoceanographic reconstructions based on Mg/Ca
391 ratios. However, more reliable estimates of past sea surface temperatures can be
392 achieved by taking into account changes in sea-ice cover. Further work on the time
393 averaging of seasonal variability in calcite chemistry is justified in order to decode
394 Southern Ocean paleoclimate records.

395

396

397 Acknowledgements:

398 The authors would like to thank the following: Damien Carson and Raja Ganeshram for DIC, pH and
399 organic carbon isotopes and useful discussion (University of Edinburgh); Norman Charnley for help
400 with stable isotope analysis ICP-MS (Department of Earth Sciences, University of Oxford); Mervyn
401 Greaves and Jimin Yu for their help with cleaning and trace metal analysis (University of Cambridge);
402 Mark Brandon (Open University), Keith Weston and Tim Jickells (University of East Anglia, Norwich)
403 for help recovering and picking the sediments; Andrew Clarke (British Antarctic Survey) and Mags
404 Wallace (Open University) for biological and physical oceanographic data; the base commander and
405 staff of Rothera Research Station and master and crew of the RRS James Clark Ross, British Antarctic
406 Survey. The authors would like to thank three anonymous reviewers for insight and discussion. The
407 work was funded as part of NERC Antarctic Funding Initiative AFI4-02. KRH is funded by NERC
408 grant NER/S/A/2004/12390.

- 409 Anand, P., Elderfield, H. and Conte, M.H., 2003. Calibration of Mg/Ca thermometry in
410 planktonic foraminifera from a sediment trap times series. *Paleoceanography*, 18:
411 1050, doi:10.1029/2002PA000846.
- 412 Anderson, R.F., Chase, Z., Fleisher, M.Q. and Sachs, J., 2002. The Southern Ocean's
413 biological pump during the Last Glacial Maximum. *Deep-Sea Research II*, 49:
414 1909-1938.
- 415 Barker, S. and Elderfield, H., 2002. Foraminiferal calcification response to glacial-
416 interglacial changes in atmospheric CO₂. *Science*, 297: 833-836.
- 417 Bauch, D., Carstens, J. and Wefer, G., 1997. Oxygen isotope composition of living
418 *Neogloboquadrina pachyderma* (sin.) in the Arctic Ocean. *Earth and Planetary Science*
419 *Letters*, 146: 47-58.
- 420 Bemis, B.E., Spero, H.J., Bijma, J. and Lea, D.W., 1998. Reevaluation of the oxygen
421 isotopic composition of planktonic foraminifera: experimental results and revised
422 paleotemperature equations. *Paleoceanography*, 13: 150-160.
- 423 Brown, S.J. and Elderfield, H., 1996. Variations in Mg/Ca and Sr/Ca ratios of planktonic
424 foraminifera caused by postdepositional dissolution: evidence of a shallow Mg-
425 dependent dissolution. *Paleoceanography*, 11: 543-551.
- 426 Clarke, A., Meredith, M.P., Wallace, M.I., Brandon, M.A. and Thomas, D.N., 2008.
427 Seasonal and interannual variability in temperature, chlorophyll and
428 macronutrients in Ryder Bay, northern Marguerite Bay, Antarctica. *Deep-Sea*
429 *Research II* (Palmer LTER Special Issue).
- 430 Darling, K.F., Kucera, M. and Wade, C.M., 2007. Global molecular phylogeography
431 reveals persistent Arctic circumpolar isolation in a marine planktonic protist.
432 *Proceeding of the National Academy of Science*, 104: 5002-5007.
- 433 Delille, B., Jourdain, B., Borges, A.V., Tison, J.-L. and Delille, D., 2007. Biogas (CO₂, O₂,
434 dimethylsulfide) dynamics in spring Antarctic fast ice. *Limnology and*
435 *Oceanography*, 52: 1367-1379.
- 436 Donner, B. and Wefer, G., 1994. Flux and stable isotope composition of *Neogloboquadrina*
437 *pachyderma* and other planktonic foraminiferas in the Southern Ocean. *Deep-Sea*
438 *Research I*, 41: 1733-1743.

439 Eggins, S., De Deckker, P. and Marshall, J., 2003. Mg/Ca variation in planktonic
440 foraminifera tests: implications for reconstructing palaeo-seawater temperature
441 and habitat migration. *Earth and Planetary Science Letters*, 212: 291-306.

442 Elderfield, H. and Ganssen, G., 2000. Past temperature and $\delta^{18}\text{O}$ of surface ocean waters
443 inferred from foraminiferal Mg/Ca ratios. *Nature*, 405: 442-445.

444 Ferguson, J.E., Henderson, G.M., Kucera, M. and Rickaby, R.E.M., 2008. Systematic
445 change of foraminiferal Mg/Ca ratios across a strong salinity gradient. *Earth and*
446 *Planetary Science Letters*.

447 Foster, G.L., 2008. Seawater pH, pCO_2 and $[\text{CO}_3^{2-}]$ variations in the Caribbean Sea over
448 the last 130 kyr: A boron isotope and B/Ca study of planktonic foraminifera.
449 *Earth and Planetary Science Letters*, 271: 254-266.

450 Gaillardet, J. and Allègre, C.J., 1995. Boron isotopic compositions of corals: seawater or
451 diagenesis record? *Earth and Planetary Science Letters*, 136: 665-676.

452 Gersonde, R., Crosta, X., Abelmann, A. and Armand, L., 2005. Sea-surface temperature
453 and sea ice distribution of the Southern Ocean at the EPILOG Last Glacial
454 Maximum - a circum-Antarctic view based on siliceous microfossil records.
455 *Quaternary Science Reviews*, 24: 869-896.

456 Gibson, J.A.E., Trull, T.W. and Nichols, P.D., 1999. Sedimentation of ^{13}C rich organic
457 matter from Antarctic sea-ice algae: a potential indicator of past sea-ice extent.
458 *Geology*, 27: 331-334.

459 Gleitz, M., Rutgers van der Loeff, M.M., Thomas, D.N., Dieckmann, G.S. and Millero,
460 F.J., 1995. Comparison of summer and winter inorganic carbon and nutrient
461 concentrations in Antarctic sea ice brine. *Marine Chemistry*, 51: 81-91.

462 Golden, K.M., Ackley, S.F. and Lytle, V.I., 1998. The percolation phase transition in sea
463 ice. *Science*, 282: 2238-2241.

464 King, A.L. and Howard, W.R., 2004. Planktonic foraminiferal $\delta^{13}\text{C}$ records from
465 Southern Ocean sediment traps: New estimates of the oceanic Suess effect.
466 *Global Biogeochemical Cycles*, 18: doi:10.1029/2003GB002162.

467 Kohfeld, K.E., Anderson, R.F. and Lynch-Stieglitz, J., 2000. Carbon isotopic
468 disequilibrium in polar planktonic foraminifera and its impact on modern and
469 Last Glacial Maximum reconstructions. *Paleoceanography*, 16: 53-64.

470 Kohfeld, K.E., Fairbanks, R.G., Smith, S.L. and Walsh, I.D., 1996. *Neogloboquadrina*
471 *pachyderma* (sinistral coiling) as paleoceanographic tracers in polar oceans:
472 evidence from northeast water polynya plankton tows, sediment traps, and
473 surface sediments. *Paleoceanography*, 11: 679.

474 Lea, D.W., Mashiotta, T.A. and Spero, H.J., 1999. Controls on magnesium and strontium
475 uptake in planktonic foraminifera determined by live culturing. *Geochimica*
476 *Cosmochimica Acta*, 63: 2369-2379.

477 Lipps, J.H. and Krebs, W.N., 1974. Planktonic foraminifera associated with Antarctic
478 sea-ice. *Journal of Foraminiferal Research*, 4: 80-85.

479 Lynch-Stieglitz, J., Stocker, T.F., Broecker, W.S. and Fairbanks, R.G., 1995. The
480 influence of air-sea exchange on the isotopic composition of oceanic carbon:
481 observations and modelling. *Global Biogeochemical Cycles*, 9: 653-655.

482 Marriott, C.S., Henderson, G.M., Belshaw, N.S. and Tudhope, A.W., 2004. Temperature
483 dependence of $\delta^7\text{Li}$, $\delta^{44}\text{Ca}$ and Li/Ca during growth of calcium carbonate. *Earth*
484 *and Planetary Science Letters*, 222: 615-624.

485 Mashiotta, T.A., Lea, D.W. and Spero, H.J., 1999. Glacial-interglacial changes in
486 Subantarctic sea surface temperature and $\delta^{18}\text{O}$ -water using foraminiferal Mg.
487 *Earth and Planetary Science Letters*, 170: 417-432.

488 Meredith, M.P. et al., 2008. Variability in the freshwater balance of northern Marguerite
489 Bay, Antarctic Peninsula: results from $\delta^{18}\text{O}$. Deep-Sea Research, SO-GLOBEC
490 Special Issue.

491 Meredith, M.P., Renfrew, I.A., Clarke, A., King, J.C. and Brandon, M.A., 2004. Impact of
492 the 1997/1998 ENSO on upper ocean characteristics in Marguerite Bay, western
493 Antarctic Peninsula. Journal of Geophysical Research, 109:
494 doi:10.1029/2003JC001784.

495 Mortyn, P.G. and Charles, C.D., 2003. Planktonic foraminiferal depth habitat and $\delta^{18}\text{O}$
496 calibrations: plankton tow results from the Atlantic sector of the Southern
497 Ocean. Paleocyanography, 18: 1037, doi:10.1029/2001PA000637.

498 Mortyn, P.G., Elderfield, H., Anand, P. and Greaves, M., 2005. An evaluation of controls
499 on planktonic foraminiferal Sr/Ca: comparison of water column and core-top
500 data from a North Atlantic transect. Geochemistry Geophysics Geosystems, 6:
501 doi:10.1029/2005GC001047.

502 Ni, Y. et al., 2007. A core top assessment of proxies for the ocean carbonate system in
503 surface-dwelling foraminifers. Paleocyanography, 22:
504 doi:10.1029/2006PA001337.

505 Nurnberg, D., 1995. Magnesium in tests of *Neogloboquadrina pachyderma* sinistral from high
506 latitude northern and southern latitudes. Journal of Foraminiferal Research, 25:
507 350-368.

508 Nurnberg, D., Bijma, J. and Hemleben, C., 1996. Assessing the reliability of magnesium
509 in foraminiferal calcite as a proxy for water mass temperatures. Geochimica
510 Cosmochimica Acta, 60: 803-814.

511 Ortiz, J.D., Mix, A.C., Rugh, W., Watkins, J.M. and Collier, R.W., 1996. Deep dwelling
512 planktonic foraminifera of the Northeast Pacific reveal environmental control of
513 oxygen and carbon isotopic disequilibria. Geochimica Cosmochimica Acta, 60:
514 4509-4524.

515 Papadimitiou, S. et al., 2007. Biogeochemical composition of natural sea ice brines from
516 the Weddell Sea during early austral summer. Limnology & Oceanography, 52:
517 1809-1823.

518 Perovich, D.K. et al., 2004. Winter sea-ice properties in Marguerite Bay, Antarctica.
519 Deep-Sea Research II, 51: 2023-2039.

520 Rosenthal, Y. et al., 2004. Interlaboratory comparison study of Mg/Ca and Sr/Ca
521 measurements in planktonic foraminifera for paleocyanographic research.
522 Geochemistry Geophysics Geosystems, 5: Q04D09,
523 doi:10.1029/2003GC000650.

524 Russell, A.D., Honisch, B., Spero, H.J. and Lea, D.W., 2004. Effects of seawater
525 carbonate ion concentration and temperature on shell U, Mg and Sr in cultured
526 planktonic foraminifera. Geochimica Cosmochimica Acta, 68: 4347-4361.

527 Sadekov, A.Y., Eggins, S.M. and De Deckker, P., 2005. Characterization of Mg/Ca
528 distributions in planktonic foraminifera species by electron microprobe mapping.
529 Geochemistry Geophysics Geosystems, 6: Q12P06, doi:10.1029/2005GC000973.

530 Sexton, P.F., Wilson, P.A. and Pearson, P.N., 2006. Microstructural and geochemical
531 perspectives on planktic foraminiferal preservation: "glassy" versus "frosty".
532 Geochemistry Geophysics Geosystems, 7: Q12P19, doi:10.1029/2006GC001291.

533 Siegenthaler, U. et al., 2005. Stable carbon cycle-climate relationship during the Late
534 Pleistocene. Science, 310: 1313-1317.

535 Sigman, D.M. and Boyle, E.A., 2000. Glacial/interglacial variations in atmospheric
536 carbon dioxide. Nature, 407: 859-869.

- 537 Simstich, J., Sarnthein, M. and Erlenjeuser, H., 2003. Paired $\delta^{18}\text{O}$ signals of
538 *Neogloboquadrina pachyderma* (s) and *Turborotalita quinqueloba* show thermal
539 stratification structure in Nordic Seas. *Marine Micropaleontology*, 48: 107-125.
- 540 Smith, L.M. et al., 2005. Temperature reconstructions for SW and N Iceland waters over
541 the last 10 cal ka based on $\delta^{18}\text{O}$ records from plankton and benthic Foraminifera.
542 *Quaternary Science Reviews*, 24: 1723-1740.
- 543 Spero, H., Bijma, J., Lea, D.W. and Bemis, B.E., 1997. Effect of seawater carbonate
544 concentration on foraminiferal carbon and oxygen isotopes. *Nature*, 390: 497-
545 500.
- 546 Spindler, M. and Dieckmann, G.S., 1986. Distribution and abundance of the planktic
547 foraminifer *Neogloboquadrina pachyderma* in sea ice of the Weddell Sea (Antarctica).
548 *Polar Biology*, 5: 185-191.
- 549 Volkman, R., 2000. Planktic foraminifers in the Outer Laptev Sea and the Fram Strait -
550 modern distribution and ecology. *Journal of Foraminiferal Research*, 30: 157-
551 176.
- 552 von Langen, P.J., Pak, D.K., Spero, H.J. and Lea, D.W., 2005. Effects of temperature on
553 Mg/Ca in neogloboquadrinid shells determined by live culture. *Geochemistry
554 Geophysics Geosystems*, 6: Q10P03, doi:10.1029/2005GC000989.
- 555 Weiss, R.F., Oestlund, H.G. and Craig, H., 1979. Geochemical studies of the Weddell
556 Sea. *Deep-Sea Research*, 26: 1093-1120.
- 557 Yu, J., Day, J., Greaves, M. and Elderfield, H., 2005. Determination of multiple
558 element/calcium ratios in foraminiferal calcite by quadrupole ICP-MS.
559 *Geochemistry Geophysics Geosystems*, 6: doi10.1029/2004GC00094.
- 560 Yu, J. and Elderfield, H., 2005. B/Ca in foraminiferal calcium carbonate and its potential
561 as a paleo-pH proxy. *Eos Trans. AGU*, 86(52) Fall meeting supplement, Abstract
562 PP11B-1451.
- 563 Yu, J., Elderfield, H. and Honisch, B., 2007. B/Ca in planktonic foraminifera as a proxy
564 for surface seawater pH. *Paleoceanography*, 22: doi:10.1029/2006PA001347.

565
566 **Figure captions:**
567

568 Figure 1: Map showing the sediment trap and RaTS site (see text for details) off the West
569 Antarctic Peninsula.

570

571 Figure 2: SEM images of foraminifera A) showing non-encrusted specimen from June; B)
572 showing encrusted specimen from May and C) an internal view showing good preservation and
573 lack of secondary calcite.

574

575 Figure 3: A) Mean surface temperature and salinity (data from British Antarctic Survey); B)
576 $\delta^{18}\text{O}_{\text{CaCO}_3}$ and $\delta^{13}\text{C}_{\text{CaCO}_3}$ results for *N. pachyderma* (s.). The hatched bar indicates the period of
577 persistent sea-ice.

578

579 Figure 4: Trace metal results for *N. pachyderma* (s.) calcite, each plotted against surface
580 temperature and salinity. The hatched bar indicates the period of persistent sea-ice.

581

582 Figure 5: A) predicted $\delta^{18}\text{O}$ of water, with values given relative to SMOW. B) Predicted $\delta^{18}\text{O}$ of
583 foraminiferal calcite. A temperature dependent vital effect between 0.6 and 1.1‰ has been
584 applied to the data.

585 The measured $\delta^{18}\text{O}_{\text{CaCO}_3}$ values can then be compared to the model to estimate habitat depths.

586 The white bars indicate the error on the $\delta^{18}\text{O}_{\text{CaCO}_3}$ measurements (0.1‰) and indicate the most
587 likely depths for calcification, and the black error bars show the error on the vital effect ($\pm 0.2\text{‰}$).

588 C) Reconstructed temperatures and salinities for the conditions at which the foraminifera calcify
589 calculated from the $\delta^{18}\text{O}$ depth profile.

590

591 Figure 6: Measures of carbonate ion concentration in seawater. A) B/Ca; B) $[\text{CO}_3^{2-}]$ calculated
592 using B/Ca and the calibration of (Yu et al., 2007). The error bars show 95% confidence
593 intervals (Equation 4); C) $[\text{CO}_3^{2-}]$ in seawater (15 m depth; black triangles) and sea-ice brine from
594 upper layers of ice collected by sackhole drilling (grey triangles), calculated using measured values
595 of alkalinity and DIC (data from Carson et al., in prep) and carbcalc 5e (Boyle, 2005); D) mean
596 shell weights for all size fractions; E) numbers of shells in each size fraction ($< 250 \mu\text{m}$ in black
597 circles; $> 250 \mu\text{m}$ in white circles) demonstrating the trends in shell weights are not a result of
598 changes in the proportion of each size fraction. The hatched box shows the period of persistent
599 sea-ice.

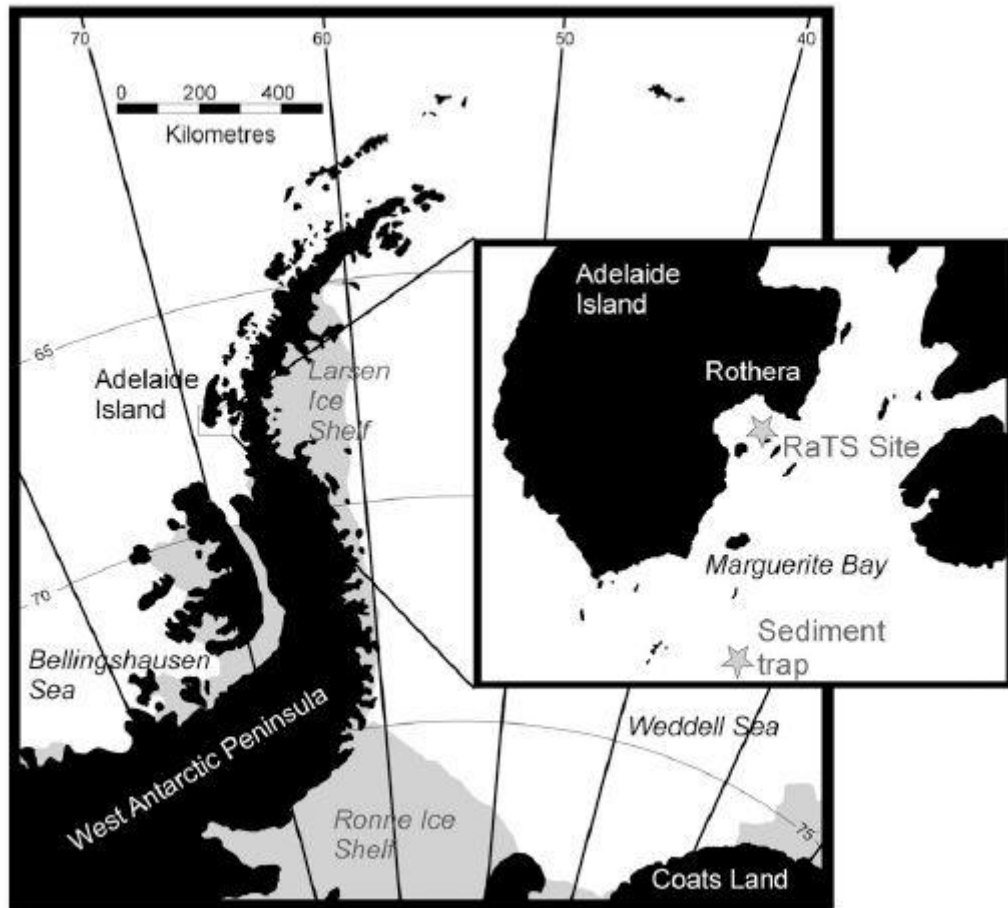
600

601 Figure 7: Controls on trace metal uptake into *N. pachyderma* (s.). A) Calcification temperature
602 and $[\text{CO}_3^{2-}]$, calculated from $\delta^{18}\text{O}_{\text{CaCO}_3}$ and B/Ca ratios respectively (Figure 3 and 4). The data
603 are smoothed using a moving average. B) Measured Mg/Ca (black triangles) and Mg/Ca
604 predicted using Equation 5 (white triangles). C) Measured Sr/Ca (black circles) and Sr/Ca

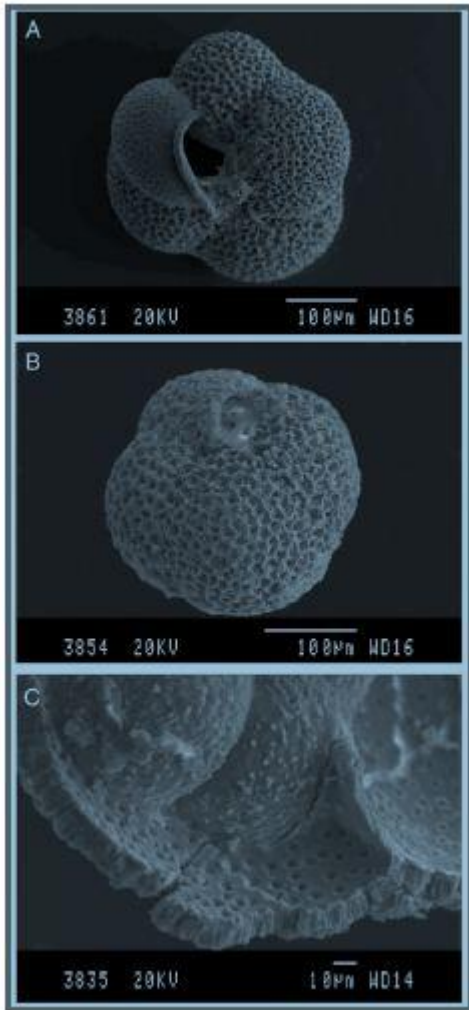
605 predicted using Equation 6 (white circles). The hatched box shows the period of persistent sea-
606 ice.

607

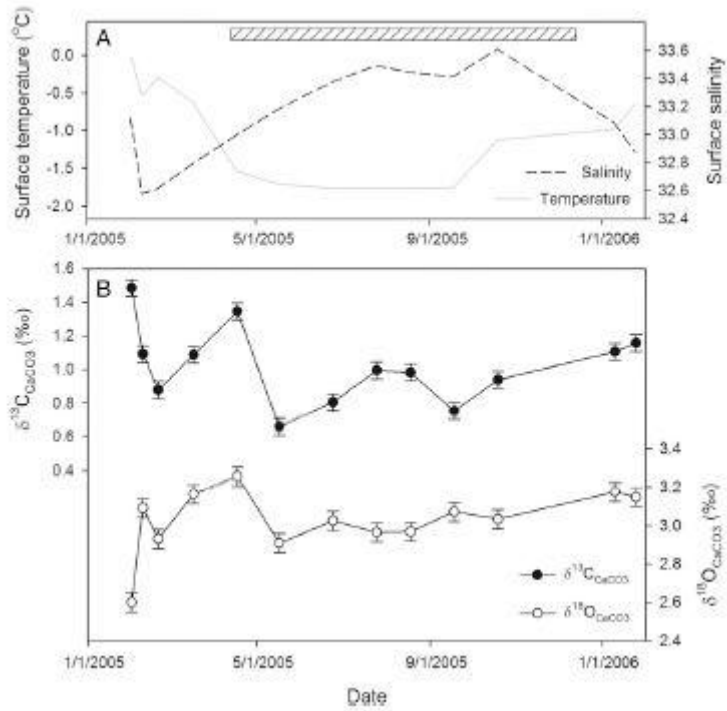
608 Figure 8: Mg/Ca residuals plotted against mean shell weight, which can be used as an
609 independent measure of $[\text{CO}_3^{2-}]$. The Mg/Ca residuals are calculated here by subtracting the
610 Mg/Ca ratio predicted using the exponential relationship given by (Elderfield and Ganssen, 2000)
611 and calcification temperature from the measured Mg/Ca value (white circles). Mg/Ca residuals
612 are also calculated here by subtracting the Mg/Ca temperature effect and constant term show in
613 Equation 5 (black circles). The Mg/Ca residuals correlate significantly with shell weight ($r^2 =$
614 0.52 , $p < 0.05$, $n = 13$).



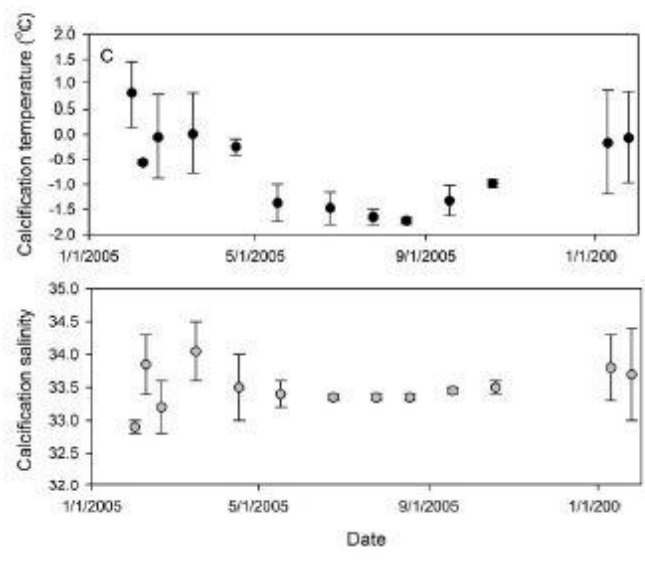
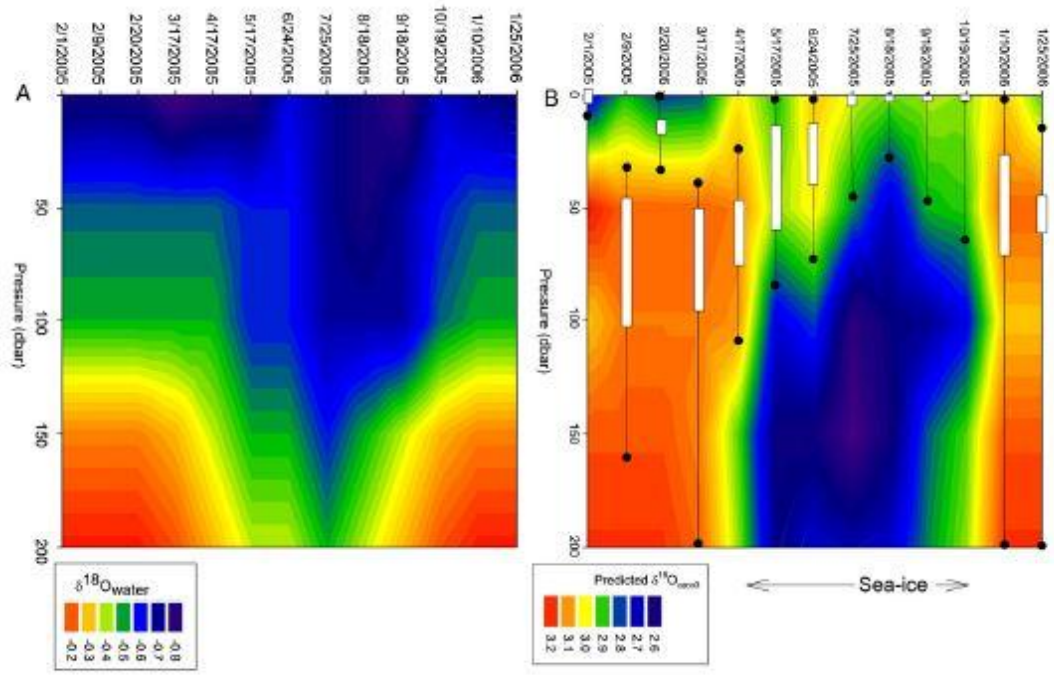
615

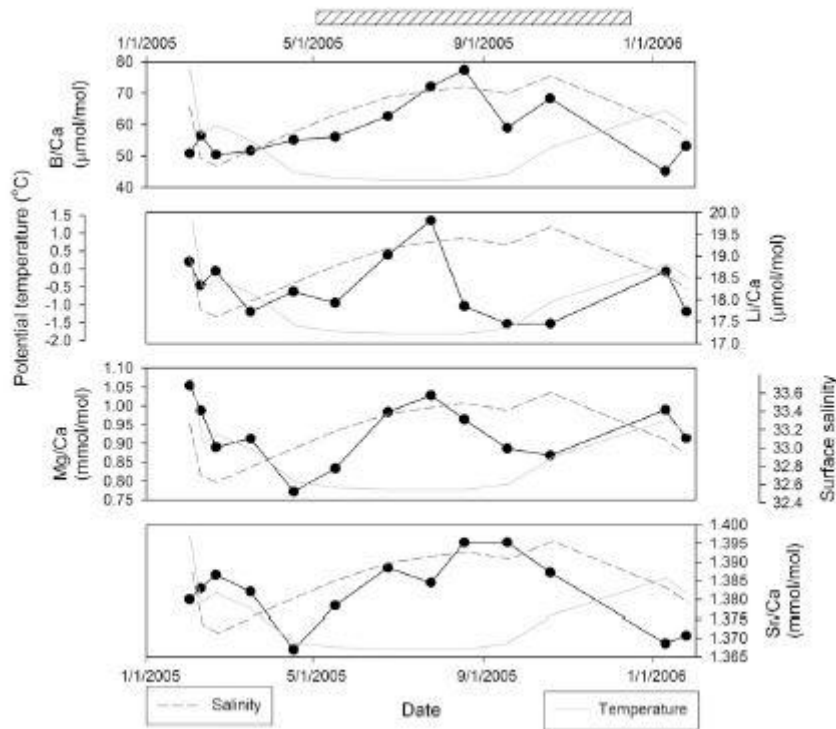


616

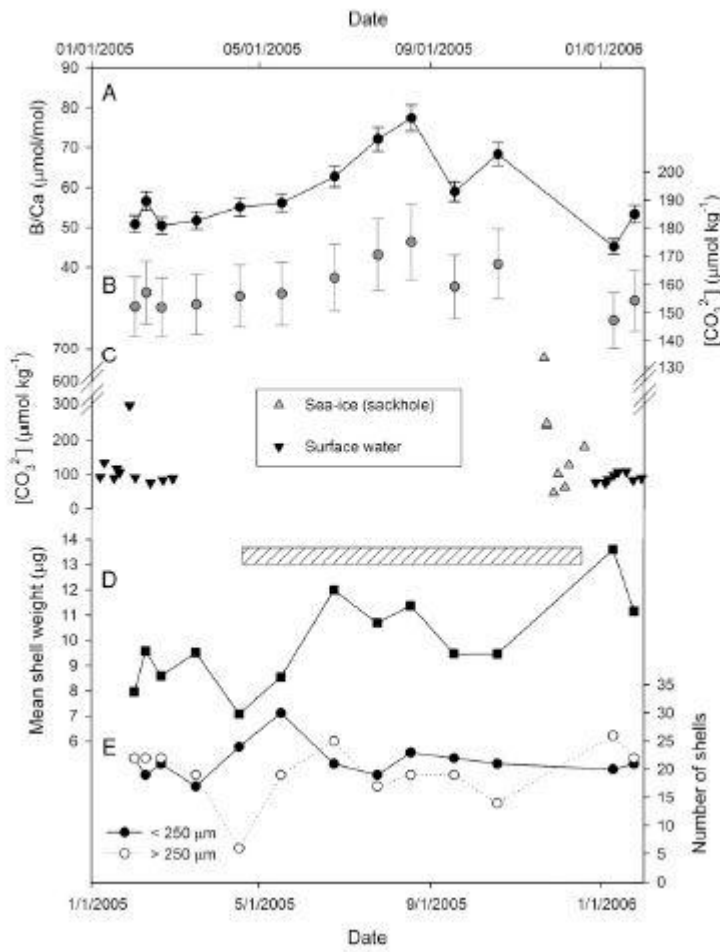


617

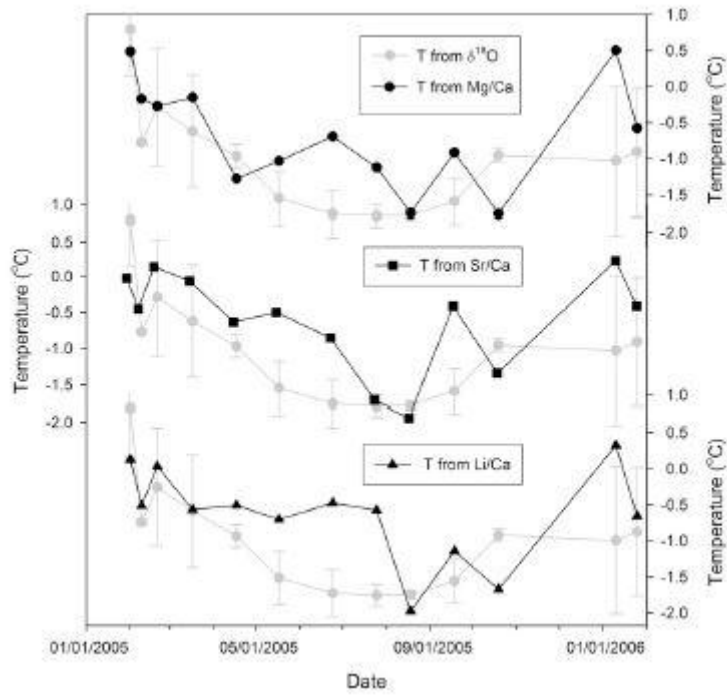




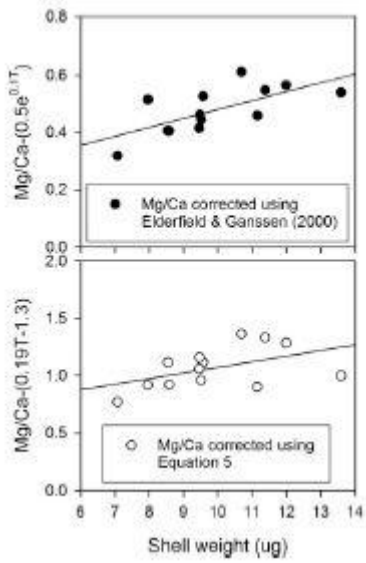
619



620



621



622